Comparison of Conventional and Modified Direct Torque Control of Three-Phase Induction Motor Using Three-Level Flying Capacitor Inverter

Amirah J. Mohammed and Raaed F. Hassan
Middle Technical University, Electrical Engineering Technical College, Baghdad, Iraq
Email: amirahalzubaidy@gmail.com; drraaed_alanbaki@mtu.edu.iq

***Abstract*—The work presented in this paper aims to compare the effectiveness of different control strategies to improve the performance of the three-phase Induction Motor (IM). The Conventional Direct Torque Control (CDTC) was employed as the first strategy for driving the IM. This control strategy causes high ripples in the IM's torque and speed due to the hysteresis comparators and a variable switching frequency due to the look-up table. A modified DTC strategy based on Space Vector Modulation (DTC-SVM) was chosen as a second strategy to enhance the performance of the IM using the two-level inverter. This method, which leads to the reduction of the torque and speed ripples and achieves constant switching frequency. As the multi-level inverter becomes most popular than the two-level inverter, the third strategy is devoted to adopting the three-level flying capacitor inverter (TLFCMLI) -based DTC-SVM. The third strategy uses the method of mapping the multi-level space vector based on basic two-level SVM. Matlab/Simulink software package is utilized to implement the suggested controllers. Simulation results show that the DTC-SVM based on TLFCMLI significantly enhances the IM's performance compared with the other two strategies from the voltage and current profiles, torque, and speed points of view.**

***Index Terms*—Direct Torque Control (DTC), Flying Capacitor Multi-Level Inverter (FCMLI), Induction Motor (IM), Modified Direct Torque Control (MDTC), Multi-Level Inverter (MLI), Space Vector Modulation (SVM)**

I. Introduction

Induction motors are the most popular electrical machines in the industry and other applications fields [1]. Its popularity is due to the low cost, reliability, and robustness compared to other motors, such as DC motors [2], [3]. The electrical machines consume most of the industries' electrical power; in this, more than two-thirds are consumed by induction motors [4]. Although the basis of induction motor work has been known since the beginning of the past century, significant progress is still being made due to advances in materials, power electronics, and high-performance microcontrollers [5], [6]. Therefore, with advanced power electronics switches and high-performance microcontrollers, induction motor drives have a competitive advantage compared to DC machines [7]. The purpose of using high-performance drivers is to fulfill the standard requirements of four-quadrant operation, minimal torque fluctuation, rapid speed recovery under load disturbances, and rapid dynamic torque and velocity responses [3], [5]. Two types of control methods for induction motors are commonly employed; are the vector control method and the Direct Torque (DTC) control method. According to its simplicity, the DTC control algorithm becomes the most popular method for controlling induction motors [5]. The DTC was first proposed in 1986 by Takahashi; this approach's principle does not need massive calculations and transformations; it consists of flux and torque estimators and a look-up table [8]–[10]. However, DTC suffers from some vital disadvantages. It presents high torque ripples, especially at the low switching frequency, producing variable switching frequency and difficulties in controlling flux and torque at the low speed [11]. Many pursuits have been proposed to overcome these drawbacks and improve DTC performance. The most widely used approach for enhancing DTC's performance has used the principle of space vector modulation and known as DTC-SVM [12]–[15]. However, modified methods to improve direct torque control with the two-level inverters' presence do not contribute sufficiently to the improvement process[16], [17]. The two-level inverters produce a non-sinusoidal output voltage which contains considerable harmonics distortion that weakens the drive performance[16]. The multi-level inverter first proposed in [18] and employed as an alternative to the conventional two-level inverters; it is utilized to reduce the harmonic of the generated voltage or current waveforms and make the inverter works in higher voltage ratings. There are three common types of multi-level inverters topologies[19], [20]; these are diode clamped multi-level inverter, flying capacitor multi-level inverter, and H-bridge multi-level inverter [21].

This paper aims to examine the effect of using the DTC-SVM on the IMs' performance compared with the conventional DTC. It also explores the benefits of using a three-level flying capacitor inverter over the conventional two-level inverter.

II. Principle of Direct Torque Control

The basic principle of the DTC is concerned with controlling the flux and torque deviations from the reference values by directly changing the inverter switching state [3].

Manuscript received May 25, 2021; revised July 16, 2021; accepted August 16, 2021.
Corresponding author: Amirah J. Mohammed (email: amirahalzubaidy@gmail.com).

doi: 10.18178/ijeetc.10.6.431-438

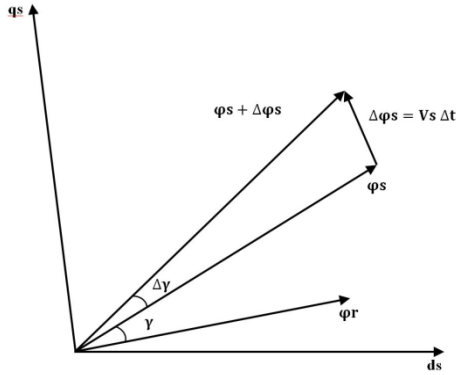

Fig. 1. Stator flux vector locus.

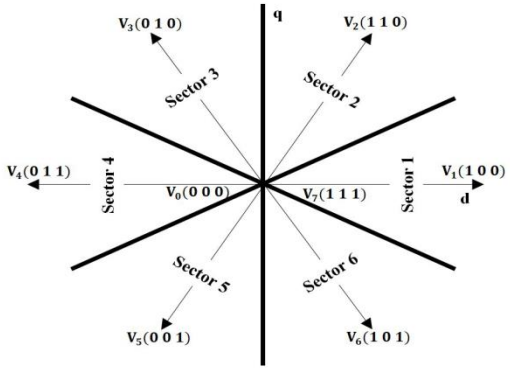

Fig. 2. Voltage vectors of the two-level inverter and sector division in the *d*-*q* plane.

The established torque can be related to the stator and rotor flux of the induction motor as follows:

$$T_e = \frac{3}{2}\frac{p}{2}\frac{L_m}{L_{\text{Ir}}L'_{\text{Is}}}|\Psi_r||\Psi_s|\sin\gamma \tag{1}$$

Furthermore, the variation of the torque will be:

$$\Delta T_e = \frac{3}{2}\frac{p}{2}\frac{L_m}{L_{\text{Ir}}L'_{\text{Is}}}|\Psi_r + \Delta\Psi_r||\Psi_s + \Delta\Psi_s|\sin\gamma \tag{2}$$

where L_{Ir} and L_{Is} are the self-inductance of the rotor and stator, respectively, L_m is the mutual inductance, $L'_{\text{Is}} = L_{\text{Ir}}L_{\text{Is}} - {L_m}^2$, and γ is the angle between Ψ_r and Ψ_s.

The assumption made to simplify (2) is that the rotor flux has no change compared with the stator flux; therefore, equation (2) will become:

$$\Delta T_e = \frac{3}{2}\frac{p}{2}\frac{L_m}{L_{\text{Ir}}L'_{\text{Is}}}|\Psi_r||\Psi_s + \Delta\Psi_s|\sin\Delta\gamma \tag{3}$$

The voltage applied to the induction motor (IM) will be represented by the following equations in a stationary reference frame [3], [20]:

$$v^s_{\text{ds}} = R_s i^s_{\text{ds}} + \frac{d}{dt}\Psi^s_{\text{ds}} \tag{4}$$

$$v^s_{\text{qs}} = R_s i^s_{\text{qs}} + \frac{d}{dt}\Psi^s_{\text{qs}} \tag{5}$$

The 1st term in (4) and (5) is the voltage drop of the stator winding; its value is minimal and can be neglected from the equations. Therefore, (4) and (5) can be written in terms of the rate of change of the stator flux as follows:

$$\frac{d\Psi_s}{dt} = V_s \quad \text{or} \quad \Delta\Psi_s = V_s\Delta t \tag{6}$$

From (7), the stator flux can be controlled using a voltage vector applied to the stator, as shown in Fig. 1.

The stator voltage vector can be determined from the following relation:

$$V_s = v_{\text{an}} + av_{\text{bn}} + a^2 v_{\text{cn}} \tag{7}$$

where $a = e^{j2\pi/3}$, v_{xn} is the phase (line-to-neutral) inverters' output voltage, and $x = a, b, c$.

In the case of a two-level inverter, the phase voltage is related to the inverters' switching state as follows:

$$v_{\text{xn}} = V_{\text{dc}}(S_x - S'_x) \tag{8}$$

where S_x and S'_x are the single-arm switching state, and they complement each other.

Substitute (8) into (7) result in:

$$V_s = V_{\text{dc}}\left[\left(S_a - S'_a\right) + a(S_b - S'_b) + a^2\left(S_c - Sc'\right)\right] \tag{9}$$

Fig. 2 shows the stator voltage vector in the *d*–*q* plane according to (9).

The basic structure of the DTC presented firstly by Takahashi [6] is shown in Fig. 3. In this approach, the induction motor's line currents and the inverters' DC voltage are employed to determine the flux and torque's instantaneous values [22].

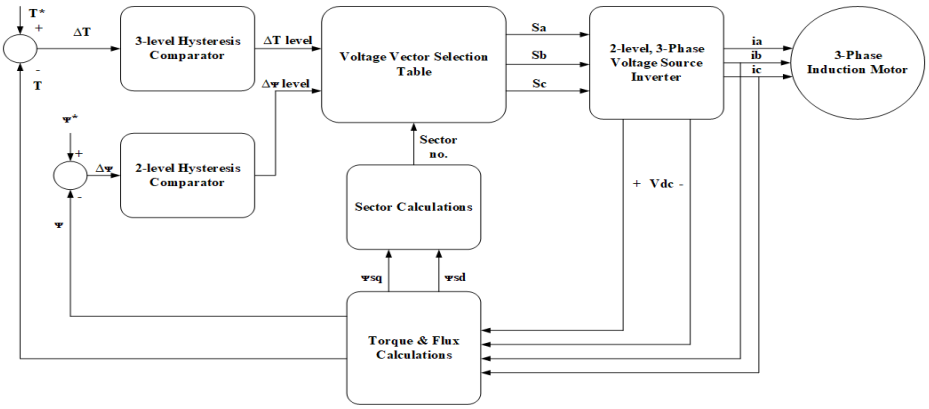

Fig. 3. Conventional DTC block diagram.

TABLE I: VOLTAGE VECTOR SELECTION (TWO-LEVEL INVERTER)

		Sectors					
$\Delta\psi$	ΔT	S_1	S_2	S_3	S_4	S_5	S_6
1	1	V2	V3	V4	V5	V6	V1
	0	V0	V7	V0	V7	V0	V7
	-1	V6	V1	V2	V3	V4	V5
-1	1	V3	V4	V5	V6	V1	V2
	0	V7	V0	V7	V0	V7	V0
	-1	V5	V6	V1	V2	V3	V4

As shown in Fig. 3, the flux and torque values are compared with the corresponding reference values. The resulting deviations of the flux and torque from their references are applied respectively to the 2-level and 3-level hysteresis comparators. The comparators' outputs and the sector calculation blocks are applied to the look-up table to determine the following sample's inverter switching state [23].

The look-up table that selects the appropriate voltage vector is shown in Table I.

III. FLYING CAPACITOR MULTILEVEL INVERTER (FCMLI)

Fig. 4 shows the basic block of a three-level one-arm flying capacitor inverter [24]-[26]. Each arm consists of four power semiconductor switches S_{1x}, S_{1x}', S_{2x}, and S_{2x}' ($x \in \{a, b, \text{and } c\}$). The switches pair ($S_{1x}$ and S_{1x}') are complementary to each other, similarly the switches pair (S_{2x} and S_{2x}') are complementary to each other. The capacitors C_1 establish the main dc-link; on the other hand, capacitor C_2 is the flying capacitor facilitating multi-level operation. The possible switching states of the three-level flying capacitor per one arm are illustrated in Table II [21]. For the three-phase configuration, the three-level inverter has 27 switching states; from this number, there are 19 active states and eight redundant states, as indicated in Fig. 5.

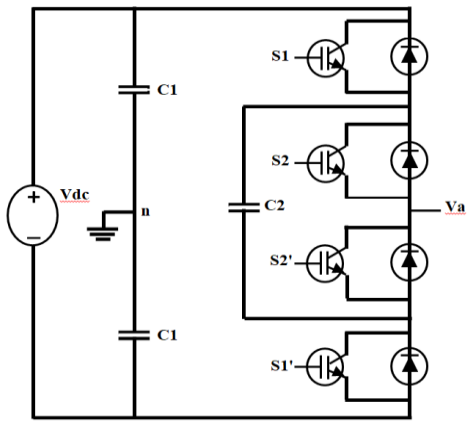

Fig. 4. One arm three-level flying capacitor inverter.

TABLE II: SWITCHING STATES OF THREE-LEVEL FLYING CAPACITOR INVERTER

S_1	S_1'	S_2	S_2'	V_{xn}
1	0	1	0	$V_{dc}/2$
1	0	0	0	0
0	1	0	0	0
0	0	1	0	0
0	0	0	1	0
0	1	0	1	$-V_{dc}/2$

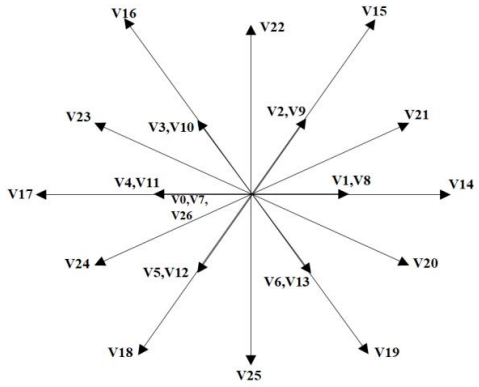

Fig. 5. Voltage vectors of the three-level flying capacitor MLI.

IV. DIRECT TORQUE CONTROL-SPACE VECTOR MODULATION (DTC-SVM)

As previously mentioned, the traditional DTC algorithm utilizes the hysteresis comparators for the torque and flux together with the sector position of the instantaneous flux to produce the appropriate switching states to the inverter. The main drawbacks associated with the hysteresis comparator are high torque and flux ripples and variable switching frequency [27], [28]. Different researchers conform to merge the advantages of the Direct Torque Control and Field Oriented Control in the same framework to overcome these drawbacks, leading to the new approach known as DTC-SVM [23] [29]. Unlike producing the switching state to the inverter based on the instantaneous values and direct calculations in the DTC, the DTC-SVM provides a switching state to the inverter based on average values and the SVM algorithm [23]. In the DTC-SVM, the reference voltage vector is estimated and is modified by the SVM technique to produce inverter switches, as shown in Fig. 6. The flow chart of the DTC-SVM is shown in Fig. 7.

In this configuration, the aim is to control the torque and flux of the induction motor. The control process is accomplished based on controlling the voltages produced by the PI controllers. The SVM block is employed to produce the switching pulses to the inverter. The DTC-SVM configuration eliminates the hysteresis controllers and the look-up table, which overcomes the drawbacks associated with them.

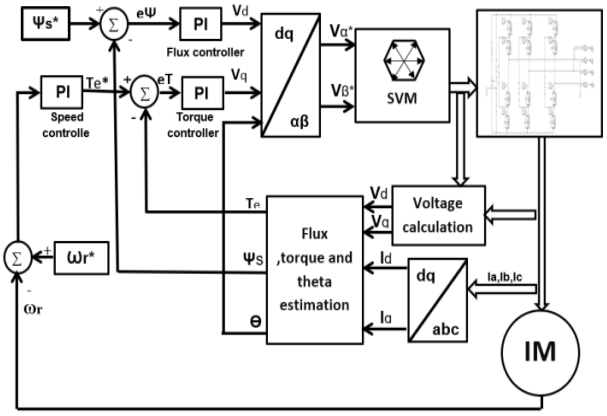

Fig. 6. DTC-SVM configuration.

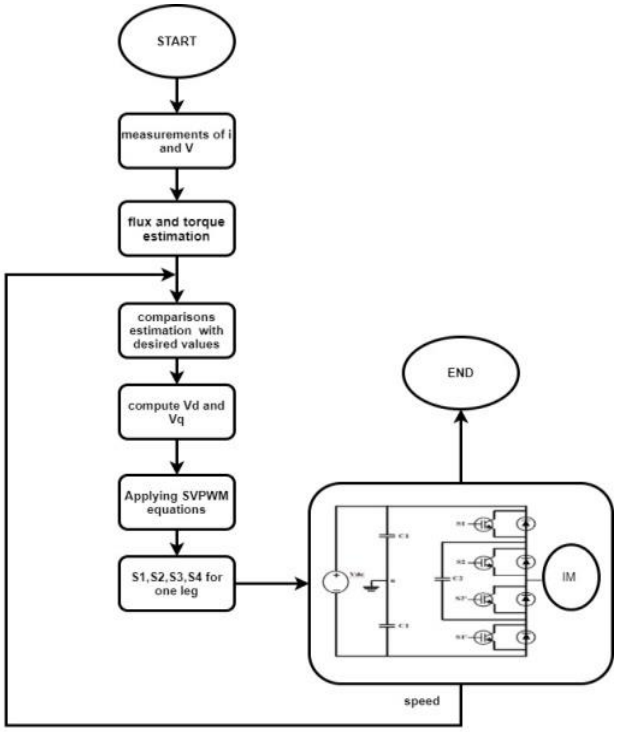

Fig. 7. Flow-chart of DTC-SVM algorithm.

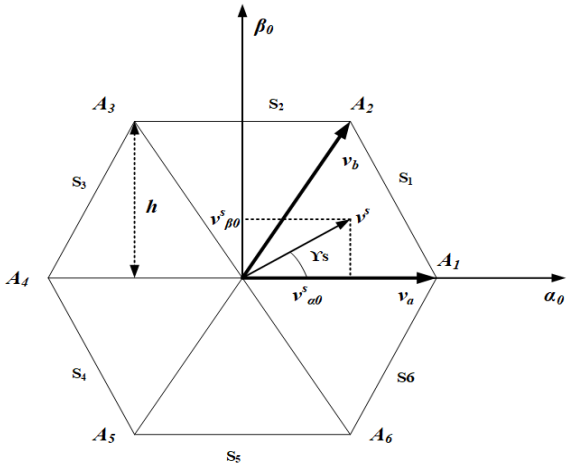

Fig. 8. Space vector of a two-level inverter.

A. DTC-SVM for Two-Level Inverter

In the case of the two-level inverter, the space vector switching aims to fit the sinusoidal reference voltage according to the six active space vectors and two zero voltage vectors produced by the inverter shown in Fig. 8 [24].

To realize the reference voltage vector $\bar{V}_s$ to its adjacent vectors with the minimum switching frequency, the total cycle T_s should be divided into three segments T_a, T_b, T_0. Using the simple geometry in Fig. 8 yields the following on-time or volt-seconds calculations:

$$\bar{V}_s T_s = T_a \bar{v}_a + T_b \bar{v}_b \tag{10}$$

where v_a=(1, 0) and v_b=(0.5, h).

$$T_a + T_b + T_0 = T_s \tag{11}$$

Take the components of $\bar{V}_s$ in quadrature axes result in:

$$v^s_{\alpha 0} T_s = t_a + 0.5 t_b \tag{12}$$

$$v^s_{\beta 0} T_s = h t_b \tag{13}$$

From (11) to (13), the on-time periods can be determined as follows:

$$T_a = T_s \left[v^s_{\alpha 0} - \frac{v^s_{\beta 0}}{2h} \right] \tag{14}$$

$$T_b = T_s \left[\frac{v^s_{\beta 0}}{h} \right] \tag{15}$$

The rest of the period will be:

$$T_0 = T_s - T_a - T_b \tag{16}$$

Fig. 9 shows the resulting leg voltage for generating reference vectors in sector 1 [30].

The sinusoidal reference space vector forms a circular path inside the hexagon. The most significant output voltage achieved with SVPWM is the radius of the largest circle inserted inside the hexagon [31].

$$\left| \bar{v}^*_s \right| = \frac{2}{3} V_{\mathrm{dc}} \cos\left(\frac{\pi}{6} \right) = \frac{1}{\sqrt{3}} V_{\mathrm{dc}} \tag{17}$$

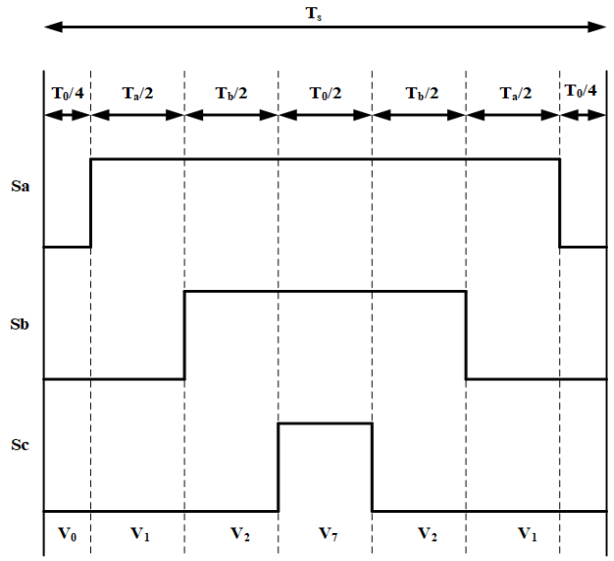

Fig. 9. Legs voltages in sector 1.

B. DTC-SVM for Three-Level Flying Capacitor Inverter

The exact configuration depicted in Fig. 6 is employed to realize the DTC-SVM algorithm for controlling IM with a three-level flying capacitor inverter. As stated in Section III, the inverter possesses 19 active switching states and eight redundant states. The space vector can be divided into six sectors, and each sector can be divided into four triangles, as shown in Fig. 9. [8]-[32].

An extension of splitting sector 1 of Fig. 10 into four triangles is shown in Fig.11, in which the reference vector A_0P of magnitude $|v^*|$ is assumed to lie in triangle Δ_3, and it makes an angle γ with the main axis α. Defining a small vector v^s in the Δ_3, which describes point P as shown in Fig. 11 (a) and (b). The volt-second required for the A_0P

is the same as that required for A_2P. The on-time calculations of the vector A_2P are similar to the on-time calculations of the two-level inverter at the specific sector. Therefore, to obtain the on-time required for any reference voltage vector in a three-level inverter, the triangle in which the reference voltage vector is located must be defined, and the components of the small vector v^s ($v^s_{\alpha 0}$ and $v^s_{\beta 0}$) is determined. The calculations of the on-time T_a, T_b, and T_0 are performed using (14)-(16).

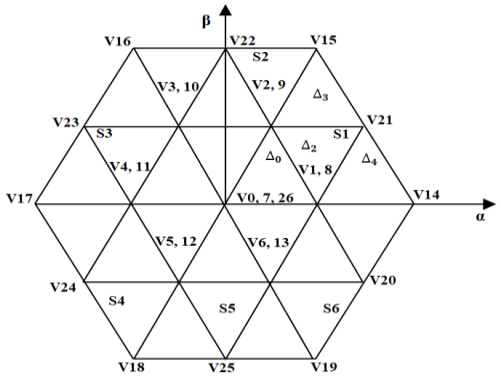

Fig. 10. Space vector of a three-level inverter.

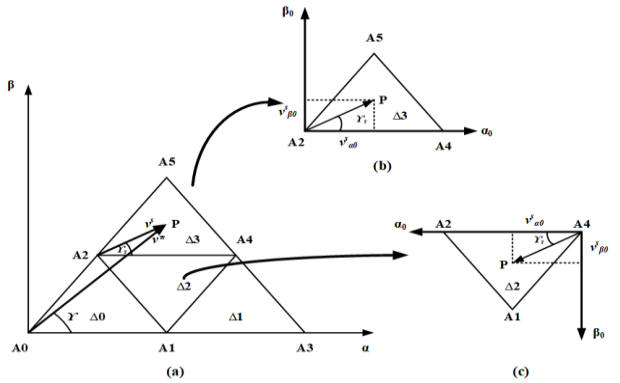

Fig. 11. Division of each sector into four triangles.

The procedure for determining the on-time switching for a three-level inverter can be summarized as follows [8]-[26].

- For the required reference vector, determine the sector S_i and γ within the sector according to the following equations:

$$S_i = \text{int}(\theta/60)+1 \tag{18}$$

$$\gamma = \text{rem}(\theta/60) \tag{19}$$

- To identify the triangle Δ_i and the small vector v^s, define two integers:

$$k_1 = \text{int}\left(v_\alpha + v_\beta/\sqrt{3}\right) \tag{20}$$

$$k_2 = \text{int}\left(v_\beta/h\right) \tag{21}$$

The map of k_1 and k_2 is shown in Fig. 12.

- Determine the components of the small vector v^s concerning virtual vertex (i.e., A1 in Fig. 12):

$$v_{\alpha i} = v_\alpha - k_1 + 0.5k_2 \tag{22}$$

$$v_{\beta i} = v_\beta - k_2 h \tag{23}$$

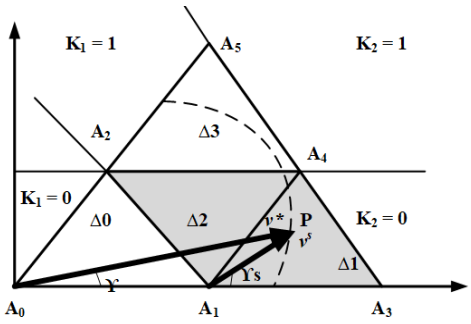

Fig. 12. Mapping of k_1 and k_2 in sector 1.

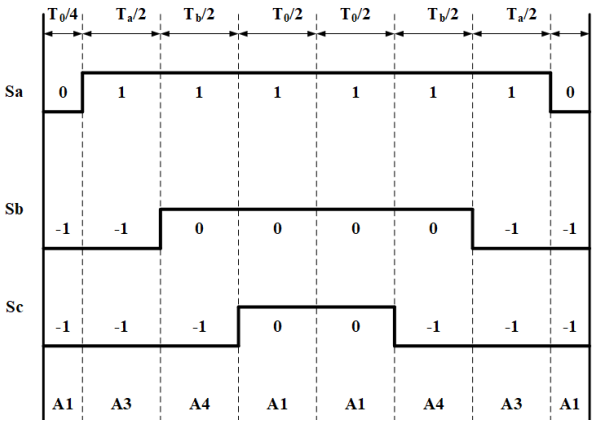

Fig. 13. Voltage of legs for reference vector at sector 1, Δ1.

- Determine the triangle number as follows:

$$\Delta_j = k_1^2 + 2k_2, \ \ j = 0,\ 1,\ \text{and}\ 3 \tag{24}$$

$$\Delta_j = k_1^2 + 2k_2 + 1, \ \ j = 2 \tag{25}$$

- Determine the on-time switching according to (14) to (16).

Fig. 13 shows the switching waveforms of the three-level inverter associated with Fig. 12.

V. Simulation Results

The simulation process based on MATLAB/Simulink has been carried out to verify the effectiveness of the designed DTC controllers on the performance of the three-phase induction motor. The parameters of the three-phase induction motor are outlined in Table III. Fig. 14 shows the simulation results of the conventional DTC-based two-level inverter, the output voltage from the inverter is shown in Fig. 14 (a), while Fig. 14 (b) shows the line current. The two-level inverter produces highly distorted phase voltage and line currents, as indicated in Fig. 14 (c) and Fig. 14 (d), representing the Total Harmonic Distortion (THD) of these parameters. Fig. 13 (e) shows the locus of the induction motor's stator flux and indicates high ripples in it. The steady-state speed and torque are shown in Fig. 14 (g) and Fig. 14 (f); respectively, it is clear they possess high fluctuations, which reduce the IM performance. The DTC-SVM is employed to drive the IM based on a two-level inverter to

examine the possibility of overcoming the drawbacks of the conventional DTC.

TABLE III: INDUCTION MOTOR PARAMETERS

Parameter			
Pole	4	L_s=L_r	0.17 H
Power	3 kW	L_m	0.16 H
Speed	1415 rpm/s	J	0.007 kg.m2
Voltage	220/380 v	Cosφ	0.89
Current	6.9 A	Roter flux	0.99wb
R_s	1.84 ohm	Frequency	5 kHz
R_r	1.84 ohm		

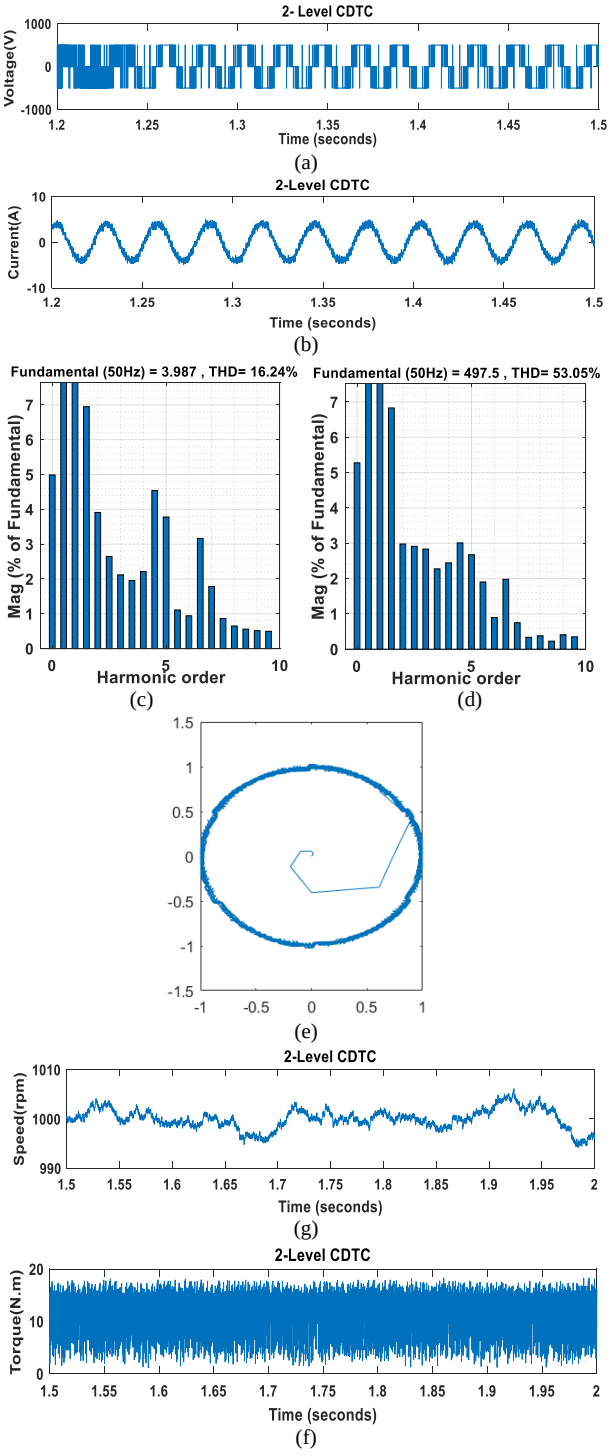

Fig. 14. Conventional DTC based two-level inverter; (a) phase voltage, (b) Line current, (c) THD of the line current, (d) THD of the phase voltage, (e) stator flux locus, (f) steady-state rotor speed, and (g) Steady-state Torque.

The simulation process is carried out for this version of the control system, and the results are shown in Fig. 15. Fig. 15 (a) shows the output phase voltage from the inverter, while Fig. 15 (b) indicates the line current. Although this approach enhances the performance of IM compared with the conventional DTC, it is also produced a highly distorted voltage and current, as shown in Fig. 15 (c) and Fig. 15 (d) for THD. The locus of the stator flux has remarkable ripples, as appear in Fig. 15 (e); the speed and torque possess high fluctuations at steady-state, as shown in Fig. 15 (g) and Fig. 15 (f).

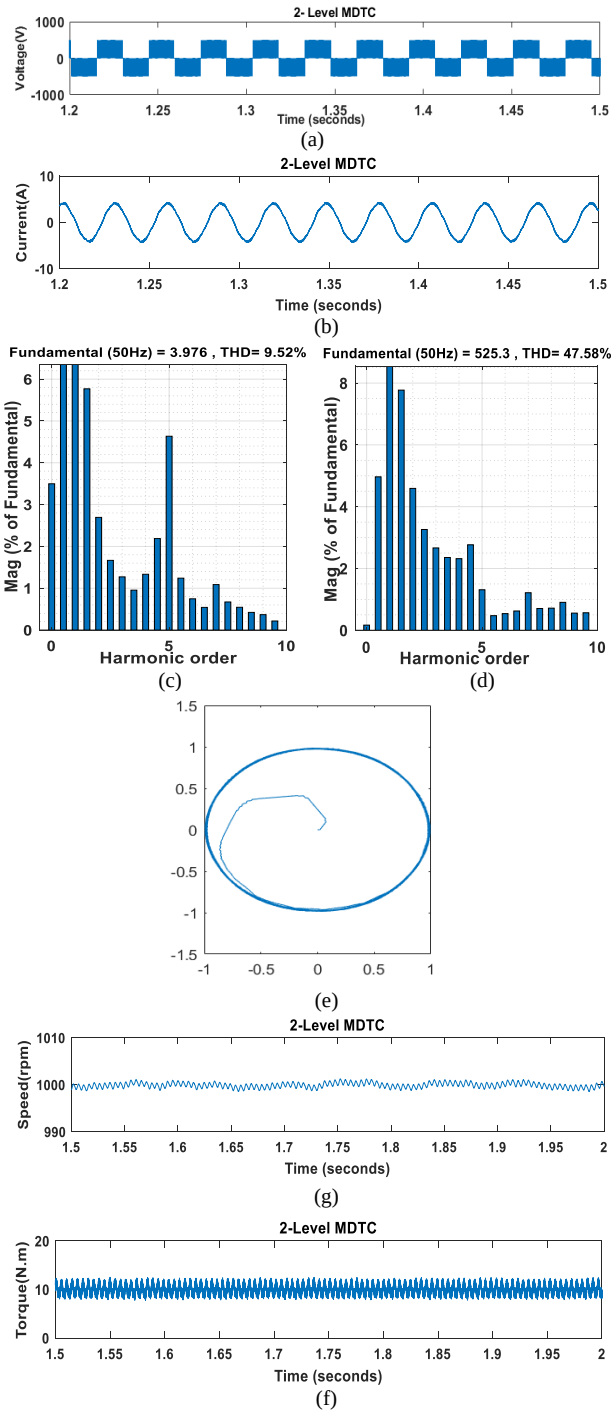

Fig. 15. Modified DTC based two-level inverter; (a) phase voltage, (b) Line current, (c) THD of the line current, (d) THD of the phase voltage, (e) stator flux locus, (f) steady-state rotor speed, and (g) Steady-state Torque.

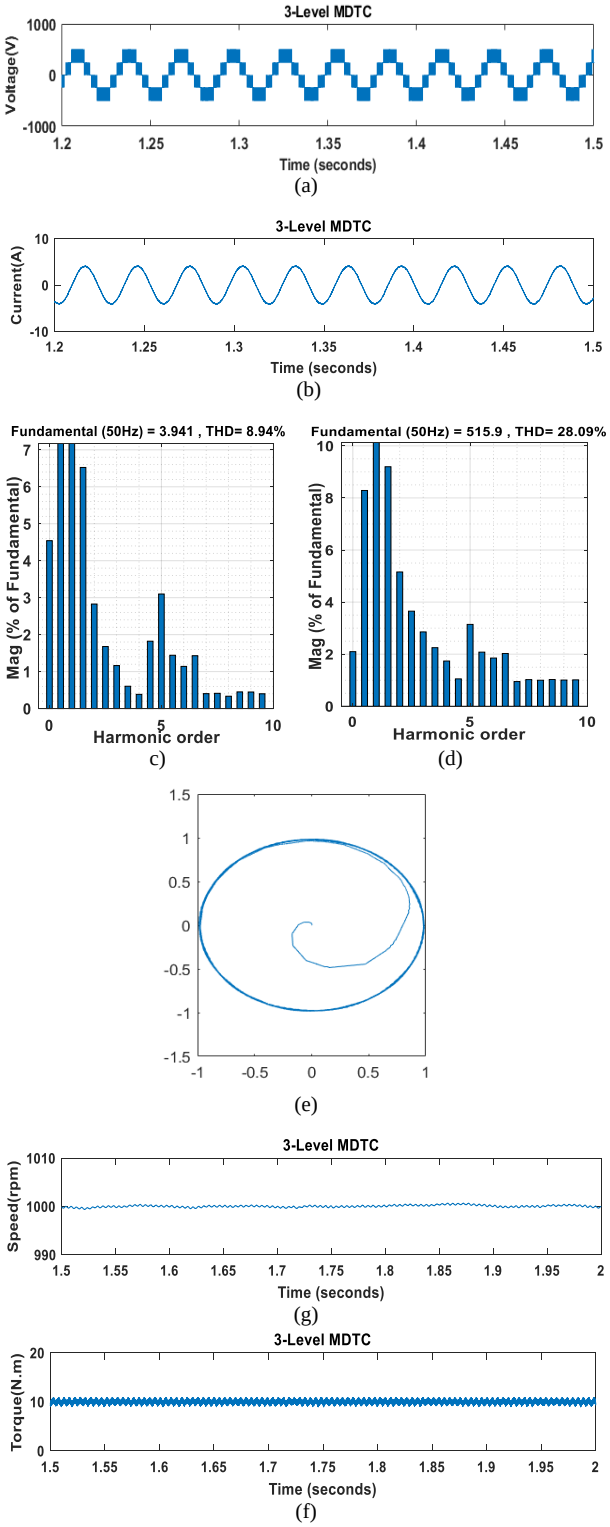

Fig. 16. Modified DTC based three-level inverter; (a) phase voltage, (b) Line current, (c) THD of the line current, (d) THD of the phase voltage, (e) stator flux locus, (f) steady-state rotor speed, and (g) Steady-state Torque.

So the comparison was made between a two-level inverter and a three-level inverter, in addition to the comparison between conventional DTC and DTC-SVM, the results were compared with this paper [10].

Significant enhancements of the IM performance have been accomplished when the DTC-SVM is employed for driving IM motor using a three-level flying capacitor inverter, as shown in Fig. 16. Fig. 16 (a) shows the phase voltage produced by the inverter, and the line current is indicated in Fig. 16 (b). The proposed control system achieves the most reduction in the harmonic distortion of the phase voltage and the line current than the previous two approaches, as shown in Fig. 16 (c) and Fig. 16 (d). The locus of the stator flux shown in Fig. 16 (e) indicates a significant reduction in the flux ripples, and the steady-state responses of the speed and torque, presented in Fig. 16 (g) and Fig. 16 (f), signify an efficient enhancement in the IM performance.

Table IV summarizes the comparison of the performance of the induction motor based on the three types of the control system presented in this paper.

TABLE IV: PERFORMANCE ANALYSIS OF THE IM BASED ON THREE TYPES OF CONTROLLERS

Load Torque = 10N·m and reference speed = 1415 RPM					
Controller	Current THD%	Voltage THD%	Speed error rpm	Torque ripple N.m	Field ripple wb
2-Level CDTC	16.24	53.05	±15	10	0.7
2-Level MDTC	9.52	47.58	±4.3	2.2	0.3
3-Level MDTC	8.94	28.09	±1.8	1.6	0.13

VI. CONCLUSION

The conventional DTC and the modified DTC (DTC-SVM) algorithms based on a two-level inverter for driving three-phase IM have been realized and verified using MATLAB/Simulink. The switching pulses produced from the conventional DTC are a function of hysteresis comparators and a look-up table. In contrast, the switching pulses produced from DTC-SVM are a function of a space vector modulation. A comparison is made between these two algorithms from the voltage and current profiles, torque, and speed responses points of view. Simulation results show that the performance of the DTC-SVM algorithm is better than that of the conventional DTC algorithm due to the absence of the hysteresis comparators and look-up table in the DTC-SVM. The effects of employing a multi-level inverter on the performance of the DTC-SVM are also considered in this paper. A DTC-SVM using a three-level flying capacitor inverter is chosen and compared with the DTC-SVM using a two-level inverter. For the TLFCMLI, the DTC-SVM is modified to determine the reference vector and on-time switching in three-level switching states based on two-level states. Although this modification leads to more complicated calculations, the simulation results indicate a significant enhancement of the system performance, which justifies this modification

CONFLICT OF INTEREST

The authors declare no conflict of interest.

AUTHOR CONTRIBUTIONS

The authors agreed with the idea of the research. The first author prepared and implemented the system designs and obtained the results under the supervision of the second author. The second author also revised the writing of the research text according to the grammatical rules.

REFERENCES

[1] M. A. Hannan, J. A. Ali, A. Mohamed, and A. Hussain, "Optimization techniques to enhance the performance of induction motor drives: A review," *Renew. Sustain. Energy Rev.*, vol. 81, no. May, pp. 1611–1626, 2018.

[2] M. Z. Niu, T. Wang, Q. Zhang, X. He, and M. L. Zhao, "A new speed control method of induction motor," in *Proc. Chinese Control Conf. CCC*, 2016, pp. 10140–10143.

[3] A. A. Adam, Y. Haroen, A. Purwadi, and A. S. Rohman, "A study of a three phase induction motor performances controlled by indirect vector and predictive torque control," in *Proc. 5th Int. Conf. Electr. Veh. Technol.*, 2018, pp. 204–209.

[4] R. Dharmaprakash and J. Henry, "Comparison of direct torque control of induction motor using two-level and three-level inverter," *Middle-East J. Sci. Res.*, vol. 23, pp. 89–96, 2015.

[5] M. A. Hannan, J. A. Ali, P. J. Ker, A. Mohamed, M. S. H. Lipu, and A. Hussain, "Switching techniques and intelligent controllers for induction motor drive: Issues and recommendations," *IEEE Access*, vol. 6, pp. 47489–47510, Aug. 2018.

[6] S. Jnayah and A. Khedher, "DTC of induction motor drives fed by two and three-level inverter: Modeling and simulation," in *Proc. 19th Int. Conf. Sci. Tech. Autom. Control Comput. Eng.*, 2019, pp. 376–381.

[7] B. V. Krishna, "Design and comparison of vector and direct torque control of 3-phase induction motor drive," *Middle - East J. Sci. Res.*, vol. 20, no. 5, pp. 586–597, 2014.

[8] I. Takahashi and T. Noguchi, "A new quick-response and high-efficiency control strategy of an induction motor," *IEEE Trans. Ind. Appl.*, vol. IA-22, no. 5, pp. 820–827, 1986.

[9] O. M. Meetei, "Advanced control methods of induction motor : A review," *ADBU Journal of Electrical and Electronics Engineering*, vol. 1, no. 1, pp. 34–40, 2017.

[10] O. Chandra Sekhar and S. Lakhimsetty, "Direct torque control scheme for a five-level multipoint clamped inverter fed induction motor drive using fractional-order PI controller," *Int. Trans. Electr. Energy Syst.*, vol. 30, no. 9, pp. 1–24, 2020.

[11] M. Vasudevan, R. Arumugam, and S. Paramasivam, "Real time implementation of viable torque and flux controllers and torque ripple minimization algorithm for induction motor drive," *Energy Convers. Manag.*, vol. 47, no. 11–12, *pp*. 1359–1371, 2006.

[12] M. Pacas and J. Weber, "Predictive direct torque control for the PM synchronous machine," *IEEE Trans. Ind. Electron.*, vol. 52, no. 5, pp. 1350–1356, 2005.

[13] A. Tripathi, A. M. Khambadkone, and S. K. Panda, "Dynamic control of torque in overmodulation and in the field weakening region," *IEEE Trans. Power Electron.*, vol. 21, no. 4, pp. 1091–1098, 2006.

[14] G. F. F. Rahman, "Foo2010.Pdf," *IEEE Aerosp. Electron. Syst. Mag.*, vol. 57, no. 1, pp. 395–403, 2010.

[15] A. R. N. I. A. Jidin, "Jidin2011.Pdf," *IEEE Trans. Ind. Electron.*, vol. 58, no. 8, pp. 3391–3400, 2011.

[16] S. E. Daoudi, L. Lazrak, N. E. Ouanjli, and M. A. Lafkih, "Improved DTC-SPWM strategy of induction motor by using five-level POD-PWM inverter and MRAS^{SF} estimator," *Int. J. Dyn. Control*, vol. 9, pp. 448-462, Jun. 2021.

[17] S. El Daoudi, L. Lazrak, and M. A. Lafkih, "Modified direct torque control for sensorless asynchronous motor fed by three-level inverter," in *Proc. 1st Int. Conf. Innov. Res. Appl. Sci. Eng. Technol.*, 2020, pp. 20–23.

[18] P. M. Bhagwat and V. R. Stefanovic, "Generalized structure of a multilevel PWM inverter," *IEEE Trans. Ind. Appl.*, vol. IA-19, no. 6, pp. 1057–1069, 1983.

[19] N. R. Das, S. C. Rai, and A. K. Nayak, "Performance analysis of heuristic optimization algorithms for demand side energy scheduling with TOU pricing," *Int. J. Eng. Technol.*, vol. 7, no. 4, pp. 3835–3842, 2018.

[20] I. E. Tashiwa, G. D. Dung, and B. S. Adole, "Review of multilevel inverters and their control techniques," *Eur. J. Eng. Res. Sci.*, vol. 5, no. 6, pp. 659–664, 2020.

[21] A. Perra, "PWM inverter technology," *IEEE Aerosp. Electron. Syst. Mag.*, vol. 7, no. 4, pp. 20–22, 1992.

[22] M. D. Islam, C. M. F. S. Reza, and S. Mekhilef, "Modeling and experimental validation of 5-level hybrid h-bridge multilevel inverter fed DTC-IM drive," *J. Electr. Eng. Technol.*, vol. 10, no. 2, pp. 574–585, 2015.

[23] S. A. A. Tarusan, A. Jidin, M. L. M. Jamil, K. A. Karim, and T. Sutikno, "A review of direct torque control development in various multilevel inverter applications," *Int. J. Power Electron. Drive Syst.*, vol. 11, no. 3, pp. 1675–1688, 2020.

[24] J. S. Lai and F. Z. Peng, "Multilevel converters-A new breed of power converters," *IEEE Trans. Ind. Appl.*, vol. 32, no. 3, pp. 509–517, 1996.

[25] J. Rodr ́guez, J. S. Lai, and F. Z. Peng, "Multilevel inverters: A survey of topologies, controls, and applications," *IEEE Trans. Ind. Electron.*, vol. 49, no. 4, pp. 724–738, 2002

[26] N. Pawar, V. K. Tayal, and P. Choudekar, "Design of flying capacitor multilevel inverter for solar energy applications," in *Proc. E3S Web Conf.*, 2020.

[27] T. G. Habetler, F. Profumo, M. Pastorelli, and L. M. Tolbert, "Direct torque control of induction machines using space vector modulation," *IEEE Trans. Ind. Appl.*, vol. 28, no. 5, pp. 1045–1053, 1992.

[28] H. Hiba, H. Ali, and H. Othmen, "DTC-SVM control for three phase induction motors," in *Proc. Int. Conf. Electr. Eng. Softw. Appl.*, 2013, vol. 1, no. 3, pp. 1–7.

[29] N. E. Ouanjli, A. Derouich, A. E. Ghzizal, *et al.*, "Modern improvement techniques of direct torque control for induction motor drives-A review," *Prot. Control Mod. Power Syst.*, vol. 4, May, 2019.

[30] F. Rashidi, "Sensorless speed control of induction motor derives using a robust and adaptive neuro-fuzzy based intelligent controller," in *Proc. IEEE Int. Conf. Ind. Technol.*, 2004, vol. 2, pp. 617–627.

[31] E. Hassankhan and D. A. Khaburi, "DTC-SVM scheme for induction motors fed with a three-level inverter," *World Acad. Sci. Eng. Technol.*, vol. 2, no. 8, pp. 168–172, 2008.

[32] A. K. Gupta and A. M. Khambadkone, "A space vector PWM scheme for multilevel inverters based on two-level space vector PWM," *IEEE Trans. Ind. Electron.*, vol. 53, no. 5, pp. 1631–1639, 2006.

Amirah J. Mohammed was born in Salah Al-Din, Iraq in 1996. She received the B.Sc. degree in electrical power engineering from Al-Furat Al-awsat Technical University, Babylon in 2017. She is currently studying M.Sc. degree in Department of Electrical Power Engineering from Middle Technical University, Baghdad.

Raaed. F. Hassan was born in Baghdad, Iraq in 1965. He received the B.Sc. degree in electrical engineering in 1986 from the Baghdad University. He received the M.Sc. and Ph.D. degrees from the University of Technology, Baghdad, Iraq in 1999 and 2006 respectively. He is currently working as a professor in the Middle Technical University, Baghdad, Iraq. He has published more than 25 papers in technical journals and conferences proceedings. His interest includes Power Electronics, Digital Signal Processing, Control, and Field Programmable Gate Array.